ABCM Symposium Series in Mechatronics - Vol. 1 - pp.311-320
Copyright © 2004 by ABCM

FINITE ELEMENT MODELING AND EXPERIMENTAL CHARACTERIZATION OF BEAMS AND PLATES TREATED WITH CONSTRAINING DAMPING LAYERS

Antonio Marcos Gonçalves de Lima
Federal University of Uberlandia - School of Mechanical Engineering - Campus Santa Monica - P. O. Box 593 - CEP 38400-902
Uberlandia - MG - Brazil
amglima@mecanica.ufu.br

Marcelo Henrique Stoppa
Federal University of Uberlandia - School of Mechanical Engineering - Campus Santa Monica - P. O. Box 593 - CEP 38400-902
Uberlandia - MG - Brazil
mhstoppa@mecanica.ufu.br

Domingos Alves Rade
Federal University of Uberlandia - School of Mechanical Engineering - Campus Santa Monica - P. O. Box 593 - CEP 38400-902
Uberlandia - MG - Brazil
domingos@ ufu.br

Abstract. *This paper is devoted to procedures for the finite element modeling of straight beams and rectangular plates treated with a surface damping treatment known as constraining damping layer, which is formed by a film of viscoelastic material inserted between the base structure and a thin metal sheet. It has been demonstrated that this type of treatment is very effective as a means of achieving vibration mitigation in various types of machines and structures. The main goal is to describe a general modeling methodology, based on finite elements, which can accommodate different treatment designs, in terms of position and extent. The frequency-dependent behavior of viscoelastic materials is introduced by means of Golla-Hughes-McTavish model, which is based on the addition of internal variables. The modeling methodology is illustrated through numerical simulations of a cantilever beam and a freely supported plate, for which analytical frequency response functions and modal properties (natural frequencies and modal damping factors) are computed from the FE matrices. Those dynamic characteristics are compared to their experimental counterparts, acquired from laboratory vibration tests. The results obtained allow to evaluate the influence of the surface treatment on the dynamic behavior of the structures considered and demonstrate the ability of the models developed in representing quite accurately such behavior.*

Keywords*. Viscoelasticity, Finite Elements, Vibration, Beams, Plates, Damping.*

1. Introduction

Passive damping approaches to the problem of vibration attenuation constitute an important subject in modern Mechanical Engineering. The application of viscoelastic materials in several engineering systems such as robots, automobiles, airplanes, communication satellites, tall buildings and space structures to reduce the vibration levels has been intensively investigated lately. Much of the knowledge available to date is compiled in the books by Nashif et al. (1985) and Mead (1998).

In the last two decades, a great deal of effort has been devoted to the development of mathematical models for the viscoelastic behavior, accounting for its dependence on operational and environmental effects, such as the excitation frequency, static preloads, dynamic loads and temperature. Some of those models are considered to be particularly suitable to be used in combination with finite element discretization, wich makes them very attractive for the modeling of real-world complex engineering systems. Among those models, it should be mentioned the so-called Fractional Derivative Model (FDM) which extends the classical standard linear model by including time derivatives of fractional order applied to stress and strain components in the viscoelastic constitutive relation. In later works (Bagley et al., 1983, 1985), FDM was incorporated into finite element models of rods and beams and complex eigenvalue and transient response analyses were illustrated through numerical simulations.

Another model developed by Golla and Hughes (1985), and McTavish and Hughes (1993), known as GHM model, is based on the introduction of dissipative variables. In Laplace domain the material modulus is represented as a partial fraction series whose terms can be interpreted as transfer functions of damped single-degree-of-freedom systems, called mini-oscillators. The GHM model leads to second-order equations of motion in standard form. As an application of the model, McTavish and Hughes (1993) describe its integration in the design of a damper strut element which transforms the extension-contraction motion of a truss element into shear deformation of the viscoelastic material, thus improving the damping effectiveness.

The model based on the Anelastic Displacement Fields (ADF) was suggested by Lesieutre and co-workers (Lesieutre, 1992; Lesieutre et al., 1996). The underlying idea is to consider the generalized displacement fields (displacements and rotations) as composed by two parts: one which accounts for the elastic part of the deformation and another accounting for anelasticity, thus associated to dissipation effects. The time evolution of the anelastic displacements is represented by a first order differential equation. As opposed to the FDM and GHM models, which are formulated in Laplace domain, the ADF model is directly formulated in the time domain.

The present paper reports part of the research work that has been carried-out by the authors aiming the development, computer implementation and numerical and experimental evaluation of passive damping systems based on the use of viscoelastic materials in different design variants. Emphasis in placed herein on the modeling of straight beams and plates treated with constraining damping layers, which are formed by viscoelastic films inserted between the base structure and a thin metal sheet. It was demonstrated that this type of treatment is much more effective in providing vibration mitigation than the simple deposition of the viscoelastic material, since the inclusion of the external metal foil allows for increased shear deformation of the viscoelastic material, thus improving energy dissipation. The frequency-dependent behavior of viscoelastic materials is introduced by means of Golla-Hughes-McTavish model. The methodology is illustrated through numerical simulations of a cantilever beam and a freely suspended plate, partially treated with passive constraining damping layers. Also, the experimental characterization of such structural elements is addressed. The model-predicted dynamic characteristics are compared to their experimental counterparts.

2. The Golla-Hughes-McTavish (GHM) viscoelastic model

According to the linear theory of viscoelasticity (Christensen, 1982), the one-dimensional stress-strain relation can be expressed, in Laplace domain, as follows:

$$\sigma(s) = G(s)\varepsilon(s) \tag{1}$$

where

$$G(s) = G_r + H(s) \tag{2}$$

In the equation above, G_r is the *static modulus*, representing the elastic behavior and $H(s)$ is the *relaxation function*, associated to the dissipation effects.

According to the GHM model (McTavish et al., 1993; Lesieutre et al., 1996), the material modulus function is expressed under the form:

$$G(s) = G_r\left(1 + \sum_{i=1}^{N_G} \alpha_i \frac{s^2 + 2\zeta_i\omega_i s}{s^2 + 2\zeta_i\omega_i s + \omega_i^2}\right) \tag{3}$$

Owing to the similarity between each term of the series appearing in Eq. (3) and the transfer function of a damped single-degree-of-freedom system, the modulus function can be interpreted as being constituted by a series of N_G mini-oscillator terms represented by three positive parameters ($\alpha_i, \omega_i, \zeta_i$).

3. Inclusion of the viscoelastic effect into finite element models

Consider the finite element equations of motion of a structure containing N degrees-of-freedom, expressed in the standard form:

$$[M]\{\ddot{q}\} + [D]\{\dot{q}\} + [K]\{q\} = \{F\} \tag{4}$$

where $[M] \in R^{N\times N}$, $[D] \in R^{N\times N}$ and $[K] \in R^{N\times N}$ denote the inertia, viscous damping and stiffness matrices, respectively, $\{q\} \in R^N$ is the vector of nodal displacements and rotations and $\{F\} \in R^N$ is the nodal load vector.

Assuming that the structure contains both elastic and viscoelastic elements, the stiffness matrix can be decomposed as follows:

$$[K] = [K_e] + [K_v(s)] \tag{5}$$

where $[K_e]$ is the stiffness matrix corresponding to the elastic substructure and $[K_v(s)]$ is the frequency-dependent stiffness matrix associated with the viscoelastic substructure. The inclusion of the frequency-dependent behavior of the viscoelastic material can be made by generating $[K_v(s)]$ for specific types of elements (rods, beams, plates, etc.) considering initially the elastic moduli E and G as being constant. Then, using the so-called *elastic-viscoelastic correspondence principle* (Christensen, 1982), those moduli are factored out of the stiffness matrix and made dependent on the frequency according to the particular viscoelastic model adopted. By assuming a constant, frequency-

independent, Poisson ratio for the viscoelastic material, $E(s)$ becomes proportional to $G(s)$ through the relation $G(s)=\dfrac{E(s)}{2(1+\nu)}$ so that a single modulus function should be used. Then, one writes:

$$\left[K_v(s)\right]=G(s)\left[\bar{K}_v\right] \tag{6}$$

Equations (3) and (6) are introduced into the Laplace-transformed Eq. (4), leading to the following system of equations of motion in Laplace domain:

$$\left[s^2[M]+s[D]+[K_e]+G_r\left[\bar{K}_v\right]\left(1+\sum_{i=1}^{N_G}\alpha_i\frac{s^2+2\zeta_i\omega_i s}{s^2+2\zeta_i\omega_i s+\omega_i^{\,2}}\right)\right]\{q(s)\}=\{F(s)\} \tag{7}$$

A series of dissipation coordinates $\{z_i\}$ $(i=1,...,N_G)$, are defined according to:

$$\{z_i(s)\}=\frac{\omega_i^{\,2}}{s^2+2\zeta_i\omega_i s+\omega_i^{\,2}}\{q(s)\} \tag{8}$$

Upon introduction of Eq. (8) into (7), after some manipulations and back transformation to time domain, the following coupled system of equations is obtained:

$$[M_G]\{\ddot{q}_G\}+[D_G]\{\dot{q}_G\}+[K_G]\{q_G\}=\{F_G\} \tag{9}$$

where:

$$[M_G]=\begin{bmatrix}[M] & 0 & \cdots & 0\\ 0 & \alpha_i\dfrac{1}{\omega_i^{\,2}}\left[K_v^0\right] & 0 & \vdots\\ \vdots & 0 & \ddots & 0\\ 0 & \cdots & 0 & \alpha_{N_G}\dfrac{1}{\omega_n^{\,2}}\left[K_v^0\right]\end{bmatrix};\ [D_G]=\begin{bmatrix}[D] & 0 & \cdots & 0\\ 0 & \alpha_i\dfrac{2\zeta_i}{\omega_i^{\,2}}\left[K_v^0\right] & 0 & \vdots\\ \vdots & 0 & \ddots & 0\\ 0 & \cdots & 0 & \alpha_{N_G}\dfrac{2\zeta_n}{\omega_n}\left[K_v^0\right]\end{bmatrix};$$

$$[K_G]=\begin{bmatrix}[K_e]+\left[K_v^\infty\right] & -\alpha_i\left[K_v^0\right] & \cdots & -\alpha_{N_G}\left[K_v^0\right]\\ -\alpha_i\left[K_v^0\right]^T & \alpha_i\left[K_v^0\right] & 0 & \vdots\\ \vdots & 0 & \ddots & 0\\ -\alpha_{N_G}\left[K_v^0\right]^T & \cdots & 0 & \alpha_{N_G}\left[K_v^0\right]\end{bmatrix};\ \{q_G\}=\left\{\{q\}^T,\{z_1\}^T,...,\{z_{N_G}\}^T\right\}^T;\ \{F\}=\left\{\{F\}^T,\{0\}^T,...,\{0\}^T\right\}^T$$

where $[M_G],\ [D_G],\ [K_G]\in R^{t_G\times t_G}$ with $t_G=N(1+N_G)$. $\left[K_v^0\right]=G_r\left[\bar{K}_v\right]$ is the static or low-frequency stiffness matrix and $\left[K_v^\infty\right]=\left[K_v^0\right]\left(1+\sum_{i=1}^{N_G}\alpha_i\right)$ is the dynamic or high-frequency stiffness matrix.

4. A three-layer sandwich beam finite element.

In this section, the formulation of a three-layer sandwich beam element is summarized, based on the original development made by Lesieutre (1992).

Figure 1 illustrates a three-node sandwich beam element of length L and width b (not indicated in the figure), which is formed by three layers: the base beam, the viscoelastic core and the constraining layer. In the same figure are also indicated the nodal degrees of freedom: transverse displacements, w_i, longitudinal displacements, u_i, cross-section rotations w'_i and shear angles of the viscoelastic layer, β.

The following assumptions are adopted:

- the base beam and the constraining layer are purely elastic with negligible transverse shear deformation. Both extensional and bending stiffness are considered, as well as transverse and rotatory cross-section inertia.
- for the viscoelastic core, classical Euler-Bernoulli hypotheses are augmented with the inclusion of a shear angle associated to transverse shear stress.

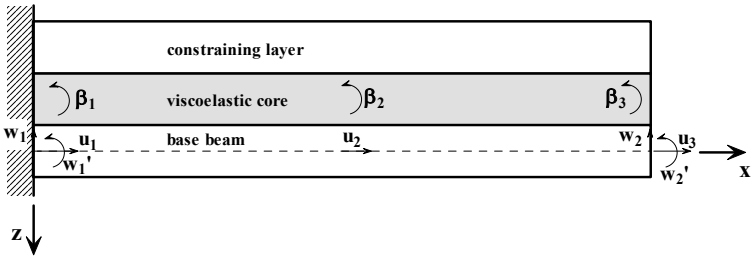

Figure 1. Three-layer sandwich beam element

The transverse displacement w is assumed to be the same for all the points lying on a same cross section and is interpolated by a cubic polynomial in x, according to:

$$w(x,t) = \left[N_w(x)\right]\left\{\bar{w}(t)\right\} \tag{10}$$

where:

$$\left[N_w(x)\right] = \left[1 - \frac{3x^2}{L^2} + \frac{2x^3}{L^3} \quad x - \frac{2x^2}{L} + \frac{x^3}{L^2} \quad \frac{3x^2}{L^2} - \frac{2x^3}{L^3} \quad -\frac{x^2}{L} + \frac{x^3}{L^2}\right] \quad \left\{\bar{w}(t)\right\} = \left[w_1(t)\; w_1'(t)\; w_2(t)\; w_2'(t)\right]^T$$

The longitudinal displacements $u_0(x,t)$ of the points lying on the middle plane of the base beam and the shear angle of the viscoelastic core β are interpolated consistently by a quadratic polynomial in x:

$$u_0(x,t) = \left[N_u(x)\right]\left\{\bar{u}(t)\right\},\ \beta(x,t) = \left[N_u(x)\right]\left\{\bar{\beta}(t)\right\} \tag{11}$$

where

$$\left[N_u(x)\right] = \left[1 - \frac{3x}{L} + \frac{2x^2}{L^2} \quad \frac{4x}{L} - 4\frac{x^2}{L^2} \quad -\frac{x}{L} + \frac{2x^2}{L^2}\right] \quad \left\{\bar{u}(t)\right\} = \left[u_1(t) \quad u_2(t) \quad u_3(t)\right]^T \quad \left\{\bar{\beta}(t)\right\} = \left[\beta_1(t) \quad \beta_2(t) \quad \beta_3(t)\right]^T$$

The strain energy accounting for extensional, bending and shear effects is given by:

$$U(t) = \frac{b}{2}\int_0^L \int_z \left(E(x,z)\varepsilon_{xx}^2 + G(x,z)\varepsilon_{xz}^2\right) dz dx \tag{12}$$

By using the strain-displacement relations:

$$\varepsilon_{xx}(x,z,t) = \frac{\partial u(x,z,t)}{\partial x},\ \varepsilon_{xz}(x,z,t) = \left(\frac{\partial u(x,z,t)}{\partial z} + \frac{\partial w(x,z,t)}{\partial x}\right)$$

and taking into account approximations (10) to (11), the development of Eq. (12) leads to:

$$U(t) = \frac{1}{2}\left\{\bar{q}(t)\right\}^T\left[K^{(e)}\right]\left\{\bar{q}(t)\right\} \tag{13}$$

where $\left\{\bar{q}(t)\right\} = \left[\left\{\bar{u}\right\} \quad \left\{\bar{w}\right\} \quad \left\{\bar{\beta}\right\}\right]^T$ is the vector of element nodal degrees-of-freedom.

The element stiffness matrix can expressed as follows:

$$\left[K^{(e)}\right] = \left[K^{(1)}\right] + \left[K^{(2)}\right] + \left[K^{(3)}\right] \tag{14}$$

where $\left[K^{(1)}\right]$, $\left[K^{(2)}\right]$ and $\left[K^{(3)}\right]$ represent, respectively, the contributions of the base beam, viscoelastic core and constraining layer to the element stiffness matrix. The expressions for theses matrices are fully developed by Lesieutre (1992).

The kinetic energy including longitudinal, transverse and cross-section rotatory motion is written:

$$T(t)=\frac{1}{2}b\int_0^L\int_z\rho(x,z)\left(\dot{w}^2+\dot{u}^2\right)dzdx \tag{15}$$

By using approximations (10) to (11), the development of Eq. (15) leads to:

$$T(t)=\frac{1}{2}\left\{\dot{\bar{q}}(t)\right\}^T\left[M^{(e)}\right]\left\{\dot{\bar{q}}(t)\right\} \tag{16}$$

where:

$$\left[M^{(e)}\right]=\left[M^{(1)}\right]+\left[M^{(2)}\right]+\left[M^{(3)}\right]$$

In the equation above, $\left[M^{(1)}\right]$, $\left[M^{(2)}\right]$ and $\left[M^{(3)}\right]$ represent, respectively, the contribution of the base beam, viscoelastic core and constraining layer to the inertia matrices. Expressions for these matrices are also provided by Lesieutre (1992).

According to Eqs. (5) and (6), the element stiffness matrix is decomposed into an elastic part $\left[K_e\right]$ and a viscoelastic part $\left[K_v\right]$ as follows:

$$\left[K_e\right]=\left[K^{(1)}\right]+\left[K^{(3)}\right],\ \left[K_v\right]=G(s)\left[\bar{K}^{(2)}\right] \tag{17}$$

5. A three-layer sandwich plate finite element

In this section the formulation of a 3-layer sandwich plate finite element is summarized based on the original development presented by Kathua e Cheung (1973).

Figure 2 depicts the plate element constituted by the base-plate, the viscoelastic core and the constraining layer, whose dimensions in directions *x* and *y* are denoted by *a* and *b*, respectively. In the remainder, superscripts (1), (2) and (3) are used to identify the quantities pertaining the base-plate, the viscoelastic core and the constraining layer, respectively.

Discretization is made by considering 4 nodes and 7 degrees-of-freedom per node, representing the longitudinal displacements of the base-plate middle plane in directions *x* and *y* (denoted by u_1 e v_1, respectively), the longitudinal displacements of the constraining layer middle plane in directions *x* and *y* (denoted by u_3 e v_3, respectively), the transverse displacement, *w*, and cross-section rotations θ_x and θ_y, about axes *x* and *y*, respectively.

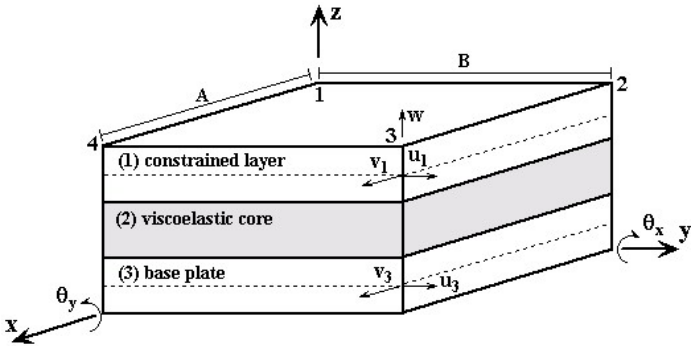

Figure 2. Three-layer sandwich plate element

The following assumptions are adopted:

- normal stresses and strains in direction *z* are neglected for all the three layers.
- the stiff layers (base-plate and constraining layer) are modeled according to Kirchhoff's theory which neglects the effects associated to transverse shear. Transverse shear is considered in the strain-state of the viscoelastic core.
- the transverse displacement *w* is the same for all the three layers and cross-section rotations about axes *x* and *y* θ_x and θ_y are assumed to be the same for the stiff layers.

The vectors of nodal and element degrees-of-freedom are defined as follows:

$$\left\{\delta^i\right\}=\left[u_1^i \quad v_1^i \quad u_3^i \quad v_3^i \quad w^i \quad \theta_x^i \quad \theta_y^i\right]^T,\ \{\delta\}=\left[\left\{\delta^1\right\}^T \quad \left\{\delta^2\right\}^T \quad \left\{\delta^3\right\}^T \quad \left\{\delta^4\right\}^T\right]^T,\ (i=1,2,3,4)$$

The longitudinal displacements are interpolated by bilinear functions of x and y whilst transverse displacements are interpolated by a third-order polynomial, as follows:

$$u_1=u_1(x,y)=a_1+a_2x+a_3y+a_4xy;\ u_3=u_3(x,y)=a_9+a_{10}x+a_{11}y+a_{12}xy$$
$$v_1=v_1(x,y)=a_5+a_6x+a_7y+a_8xy;\ v_3=v_3(x,y)=a_{13}+a_{14}x+a_{15}y+a_{16}xy$$
$$w=w(x,y)=b_1+b_2x+b_3y+b_4x^2+b_5xy+b_6y^2+b_7x^3+b_8x^2y+b_9xy^2+b_{10}y^3+b_{11}x^3y+b_{12}xy^3$$

By evaluating the equations above at each of the four nodes, the interpolation relations are obtained under the following forms:

$$u_1=\left[N_{u_1}\right]\{\delta\};\ v_1=\left[N_{v_1}\right]\{\delta\};\ u_3=\left[N_{u_3}\right]\{\delta\};\ v_3=\left[N_{v_3}\right]\{\delta\};$$
$$w=\left[N_w\right]\{\delta\};\ \theta_x=\frac{\partial}{\partial x}\left[N_w\right]\{\delta\};\ \theta_y=\frac{\partial}{\partial y}\left[N_w\right]\{\delta\} \tag{18}$$

The longitudinal displacements of the viscoelastic core middle plane in directions x and y are related to the corresponding quantities pertaining the two other layers through the following equations:

$$u_2=\frac{1}{2}\left[u_1+u_3+\frac{h_1-h_3}{2}\frac{\partial w}{\partial x}\right];\ v_2=\frac{1}{2}\left[v_1+v_3+\frac{h_1-h_3}{2}\frac{\partial w}{\partial y}\right]$$

Based on the above-mentioned hypotheses concerning the stress state of the layers, the following stress-strain relations are written:

- For the base plate:

$$\begin{Bmatrix}\sigma_x^{(1)}\\ \sigma_y^{(1)}\\ \tau_{xy}^{(1)}\end{Bmatrix}=\begin{bmatrix}\frac{E^{(1)}}{1-\nu^{(1)^2}} & \frac{E^{(1)}\nu^{(1)}}{1-\nu^{(1)^2}} & 0\\ \frac{E^{(1)}\nu^{(1)}}{1-\nu^{(1)^2}} & \frac{E^{(1)}}{1-\nu^{(1)^2}} & 0\\ 0 & 0 & G^{(1)}\end{bmatrix}\begin{Bmatrix}\varepsilon_x^{(1)}\\ \varepsilon_y^{(1)}\\ \gamma_{xy}^{(1)}\end{Bmatrix}\ \text{or}\ \left\{\sigma^{(1)}\right\}=\left[E^{(1)}\right]\left\{\varepsilon^{(1)}\right\}=\left[E^{(1)}\right]\left[D^{(1)}\right]\{\delta\} \tag{19}$$

- For the viscoelastic core:

$$\begin{Bmatrix}\sigma_x^{(2)}\\ \sigma_y^{(2)}\\ \tau_{xy}^{2}\\ \tau_{xz}^{2}\\ \tau_{yz}^{2}\end{Bmatrix}=\begin{bmatrix}\frac{E^{(2)}}{1-\nu^{(2)^2}} & \frac{E^{(2)}\nu^{(2)}}{1-\nu^{(2)^2}} & 0 & 0 & 0\\ \frac{E^{(2)}\nu^{(2)}}{1-\nu^{(2)^2}} & \frac{E^{(2)}}{1-\nu^{(2)^2}} & 0 & 0 & 0\\ 0 & 0 & G^{(2)} & 0 & 0\\ 0 & 0 & 0 & G^{(2)} & 0\\ 0 & 0 & 0 & 0 & G^{(2)}\end{bmatrix}\begin{Bmatrix}\varepsilon_x^{(2)}\\ \varepsilon_y^{(2)}\\ \gamma_{xy}^{2}\\ \gamma_{xz}^{2}\\ \gamma_{yz}^{2}\end{Bmatrix}\ \text{or}\ \left\{\sigma^{(2)}\right\}=\left[E^{(2)}\right]\left\{\varepsilon^{(2)}\right\}=\left[E^{(2)}\right]\left[D^{(2)}\right]\{\delta\} \tag{20}$$

- For the constraining layer:

$$\begin{Bmatrix}\sigma_x^{(3)}\\ \sigma_y^{(3)}\\ \tau_{xy}^{(3)}\end{Bmatrix}=\begin{bmatrix}\dfrac{E^{(3)}}{1-\nu^{(3)^2}} & \dfrac{E^{(3)}\nu^{(3)}}{1-\nu^{(3)^2}} & 0\\ \dfrac{E^{(3)}\nu^{(3)}}{1-\nu^{(3)^2}} & \dfrac{E^{(3)}}{1-\nu^{(3)^2}} & 0\\ 0 & 0 & G^{(3)}\end{bmatrix}\begin{Bmatrix}\varepsilon_x^{(3)}\\ \varepsilon_y^{(3)}\\ \gamma_{xy}^{(3)}\end{Bmatrix} \text{ or } \left\{\sigma^{(3)}\right\}=\left[E^{(3)}\right]\left\{\varepsilon^{(3)}\right\}=\left[E^{(3)}\right]\left[D^{(3)}\right]\{\delta\} \tag{21}$$

where $\left[D^{(k)}\right]$ (k = 1,2,3) denote matrices formed by derivatives of the shape functions according to the strain-displacement relations.

The strain energy for the sandwich plate is written as:

$$U=\sum_{k=1}^{3}U^{(k)} \tag{22}$$

where:

$$U^{(k)}=\frac{1}{2}\int_V\left(\left\{\sigma^{(k)}\right\}^T\left\{\varepsilon^{(k)}\right\}\right)dV \tag{23}$$

By introducing Eqs. (19) to (21) into (23), the strain energy for the composite element is expressed in terms of the element degrees-of-freedom as follows:

$$U=\frac{1}{2}\sum_{k=1}^{3}\{\delta\}^T\left[K^{(k)}\right]\{\delta\} \tag{24}$$

where $\left[K^{(k)}\right]=\int_V\left(\left[D^{(k)}\right]^T\left[E^{(k)}\right]\left[D^{(k)}\right]\right)dV$ indicates the stiffness matrix associated to the k-th layer.

Similarly, the kinetic energy of the composite plate element is expressed as the sum of the kinetic energies of the component layers:

$$T=\sum_{k=1}^{3}T^{(k)}$$

where:

$$T^{(k)}=\frac{1}{2}\rho_k h_k\int_A\left(\dot{w}+\dot{u}_k^2+\dot{v}_k^2\right)dA \tag{25}$$

By introducing the interpolation relations (18) into (25), the kinetic energy of the plate element can be expressed as follows:

$$T=\frac{1}{2}\sum_{k=1}^{3}\left\{\dot{\delta}\right\}^T\left[M^{(k)}\right]\left\{\dot{\delta}\right\}$$

where:

$$\left[M^{(k)}\right]=\rho_k h_k\int_A\left(\left[N_w\right]^T\left[N_w\right]+\left[N_{u_k}\right]^T\left[N_{u_k}\right]+\left[N_{v_k}\right]^T\left[N_{v_k}\right]\right)dA$$

According to Eqs. (5) and (6), the element stiffness matrix is decomposed into an elastic part $\left[K_e\right]$ and a viscoelastic part $\left[K_v\right]$ as follows:

$$\left[K_e\right]=\left[K^{(1)}\right]+\left[K^{(3)}\right],\ \left[K_v\right]=G(s)\left[\bar{K}^{(2)}\right]$$

The assembling of element matrices into global matrices follows the standard procedure based on the connection of neighborg elements through nodes.

6. Experimental procedure.

To validate the modeling procedures, experimental tests were performed on a cantilever beam and a freely suspended plate, both made of aluminum, treated with constraining damping layers made of a thin layer of viscoelastic material 242F01 manufactured by 3M^{TM} and an outer thin aluminum sheet.

The experimental tests consisted in obtaining a set of frequency response functions (of both driving point and transfer types) corresponding to a previously select set of points, by applying impact excitations with a modal hammer in the direction perpendicular to the specimen surface and measuring the corresponding time domain accelerations in the same direction by using a piezoelectric accelerometer. The average FRFs over 20 samples were then computed by using a spectrum analyzer. Among the various setup parameters concerning data acquisition and processing, it is important to mention that rectangular windowing was used so as to ensure that actual damping ratios, provided exclusively by the viscoelastic treatment, could be obtained.

Several configurations were tested, each one corresponding to a given position and extent of surface treatment. In the following, only one treatment configuration is being presented for each test item, as illustrated in Figure 3. Also, the base structures (without surface damping treatment) were tested and their FRFs recorded to be used as reference data in evaluating the influence of the surface treatment on the dynamic characteristics.

7. Beam and plate finite element models.

Figure 3 depicts the finite element models which have been implemented, based on the theory presented in Sections 4 and 5, to model the behavior of the beam and plate. Table 1 provides the values of the physical and geometrical properties used to generate the FE models. In Table 2 one can find the parameters of the six mini-oscillator-GHM model for the material 242F01, identified from curve fitting of the data provided by the manufacturer. Details of the identification procedure can be found in (Lima et al, 2003).

Table 1. Physical and geometrical characteristics of the beam and plate FE models

<table>
<tr><th colspan="3">Beam</th><th colspan="3">Plate</th></tr>
<tr><th>Base-beam</th><th>Viscoelastic core</th><th>Constraining layer</th><th>Base-plate</th><th>Viscoelastic core</th><th>Constraining layer</th></tr>
<tr><td>L = 0,5 m
b =38×10^{-3} m</td><td>L = 0,5 m
b =38×10^{-3} m</td><td>L = 0,5 m
b =38×10^{-3} m</td><td>A = 20×10^{-2} m
B = 25×10^{-2} m</td><td>C =2×10^{-2} m</td><td>C =2×10^{-2} m</td></tr>
<tr><td>h_b = 45×10^{-4} m</td><td>h_v = 20x10^{-5} m</td><td>h_c = 5x10^{-4} m</td><td>h_p = 3×10^{-3}m</td><td>h_v = 20x10^{-5} m</td><td>h_c = 5x10^{-4} m</td></tr>
<tr><td>E = 70,3×10^9 N/m</td><td rowspan="2">ρ = 1099,5 Kg/m^3
ν = 0,5</td><td>E = 70,3×10^9 N/m</td><td>E = 70,3×10^9 N/m</td><td rowspan="2">ρ = 1099,5 Kg/m^3
ν = 0,5</td><td>E = 70,3×10^9 N/m</td></tr>
<tr><td>ρ = 2750 Kg/m^3</td><td>ρ = 2750 Kg/m^3</td><td>ρ = 2750 Kg/m^3</td></tr>
</table>

Table 2. Parameters of the GHM viscoelastic model identified for material 3M^{TM} 242F01.

Mini-oscillator	1	2	3	4	5	6
αi	1,047	5,524	1,589	10,330	59,999	163,130
ζ_i	3911,898	323,891	48,414	30,544	14,627	4,763
ω_I [rad/s]	4943,062	6577,256	56363,554	45473,430	8601,413	57841,215
G_r [MPa]	0,079					

8. Analytical and experimental results

Figures 4(a) e 4(b) present the amplitudes of the FRFs calculated from the finite element models, compared to the experimentally acquired counterparts. The finite element FRFs where computed by direct inversion of the dynamic stiffnness matrix, as follows:

$$H = \left(\left[K_G \right] + i\omega \left[D_G \right] - \omega^2 \left[M_G \right] \right)^{-1} \tag{26}$$

All the computation were carried out in MATLAB^{TM} environment.

For the beam and plate, these FRFs are the driving-point FRFs associated with point P and I, respectively, whose positions are indicated on Figure 3. Tables 3 and 4 enable to compare the values of the FE-predicted and experimentally acquired natural frequencies and modal damping factors. Both sets were obtained by using the well-known Half-Power-Bandwidth method (Nashif *et. al.,* 1985).

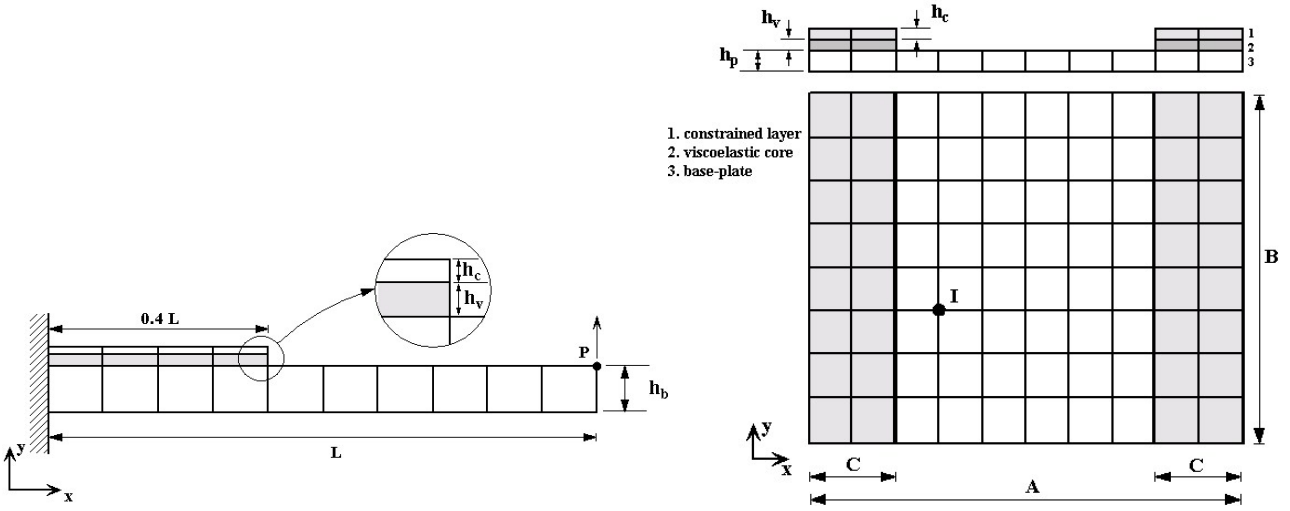

Figure 3. Illustration of the FE models implemented for the beam and plate with partial surface treatment

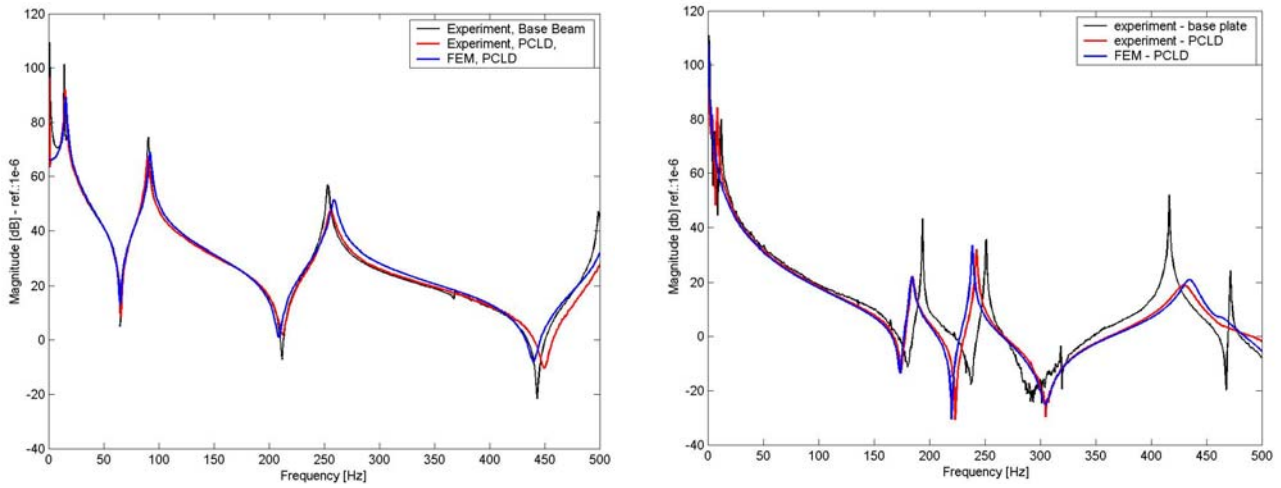

(a) (b)

Figure 4. Amplitudes of FE and experimental FRFs. (a) beam and (b) plate

Table 3. FE and experimental natural frequencies and modal damping factors of the beam

Mode	**1**		**2**		**3**	
Modal parameters	**ω_1 (Hz)**	**ζ_1**	**ω_2 (Hz)**	**ζ_2**	**ω_3 (Hz)**	**ζ_3**
Experimental	15,20	$2{,}87\times10^{-2}$	90,10 Hz	$1{,}01\times10^{-2}$	256,16 Hz	$1{,}04\times10^{-2}$
FE	15,64	$2{,}82\times10^{-2}$	91,99 Hz	$9{,}13\times10^{-3}$	259,07 Hz	$9{,}24\times10^{-3}$
Deviations (%)	2,89	1,77	2,10	10,62	1,14	12,55

Table 4. FE and experimental natural frequencies and modal damping factors of the plate

Mode	**1**		**2**		**3**	
Modal parameters	**ω_1 (Hz)**	**ζ_1**	**ω_2 (Hz)**	**ζ_2**	**ω_3 (Hz)**	**ζ_3**
Experimental	184,37	$8{,}1\times10^{-3}$	242,47	$1{,}9\times10^{-3}$	429,38	$18{,}2\times10^{-3}$
FE	184,38	$7{,}5\times10^{-3}$	238,75	$1{,}8\times10^{-3}$	434,4	$14{,}4\times10^{-3}$
Deviations (%)	0,00	8,00	1,60	5,50	1,30	26,40

9. Discussion

The analytical and experimental results presented above enable to evaluate the influence of the surface damping treatment on the dynamic behavior of the beam and plate specimens. A particular aspect to be pointed-out is the ability demonstrated by the FE models to represent the characteristic frequency-dependent behavior of the viscoelastic material. In terms of vibration attenuation, it can be observed in Figure 4 that the damping treatment provided

significant decrease in the amplitudes of the resonance peaks for both structures. By comparing the analytical and experimental results it can be noticed that the two sets are resonably close to each other. The observed deviations can have been originated in both the FE modeling and experimental tests. Clearly, as expected, differences between the values of damping ratios are found to be larger than those pertaining the natural frequencies. It is thought that some possible sources of error are:

- uncertainties in the process of collecting the numerical values of experimental data provided by the manufacturer of the viscoelastic material in the form of log-scale curves;
- residual errors in the identification of the GHM parameters from experimental data.
- assumptions, in the FE modeling, of ideal conditions for the application of the surface treatment, such as perfect adhesion and boundary conditions.
- erros in the estimation of physical and geometrical properties used to generate the FE models (Young moduli, mass density, geometrical dimensions).
- influence of temperature oscillations on the behavior of the viscoelastic material during tests.
  influence of low frequency-resolution on the estimated values of modal damping factors estimated from the FRFs.

10. Concluding remarks

Finite element models of two-dimensional beams and plates treated with passive constraining damping layers have been implemented and validated by experimental tests. The implemented modeling procedure was conceived so as to encompass different designs, regarding the position and extent of the surface treatment. The Golla-Hughes-McTavish model was used to include the frequency-dependent viscoelastic behavior in the model, proving to be an efficient strategy, in spite of the significant increase it leads in the order of the system's state matrices. Moreover, the GHM model leads to a state-space model in the time domain, which can be numerically solved to perform time-response, eingenvalue and frequency response analyses by employing standard numerical procedures.

Taking into account the existence of modeling and experimental sources of errors, some of which could be hardly avoided, the differences between the experimental and FE-predicted FRFs and modal quantities are considered to be small enough to enable to conclude about the effectiveness of the FE models in representing the dynamic behavior of beam and plates treated with passive constraining damping layers.

11. Acknowledgements

A.M.G. Lima and M.H. Stoppa thank agency CAPES for the grant of graduate scholarships. D.A. Rade is gratefull to CNPq for the support to his research activities through project 520418/98-0. The authors thank 3M do Brasil for having provided samples of viscoelastic materials used in the experimental tests. They are also gratefull to undergraduate student Luiz Alberto Carvalho Fernandes for his valuable help in the laboratory tests.

12. References

Bagley, R. L. and Torvik, P. J., 1983, "Fractional Calculus – A Different Approach to the Analysis of Viscoelastically Damped Structrures", AIAA Journal, 21 (5), pp. 741-748.

Bagley, R. L. and Torvik, P. J., 1985, "Fractional Calculus in the Transient Analysis of Viscoelasticity Damped Strucutres", AIAA Journal, 23 (6), pp. 918-925.

Christensen, R. M., 1982, "Theory of Viscoelasticity: An Introduction", Academic Press, Inc.

Golla, D. F. and Hughes, P. C., 1985, "Dynamics of Viscoelastic Structrures – A Time-Domain, Finite Element Formulation", Journal of Applied Mechanics, Vol 52, pp. 897-906.

Khatua, T. P. and Cheung, Y. K., 1973, "Bending and Vibration of Multilayer Sandwich Beams and Plates", Int. Journal for Numerical Methods in Eng., Vol. 6, pp. 11-24.

Lesieutre, G. A., 1992, "Finite Elements for Dynamic Modeling of Uniaxial Rods With Frequency-Dependent Material Properties", Int. J. Solids. Structures, Vol 29, No. 12, pp. 1567-1579.

Lesieutre, G. A. and Lee, U., 1996, "A Finite Element for Beams Having Segmented Active Constrained Layers With Frequency-Dependent Viscoelastics", Smart Mater. Struct. 5, pp. 615-627.

Lima, A. M. G., Stoppa, M. H. and Rade, D. A., 2003, "Finite Element Modeling of Structures Incorporating Viscoelastic Materials", Proceedings to XXI IMAC, Hyatt Orlando: Kissimmee, Florida.

McTavish, D. J. and Hughes, P. C., 1993, "Modelling of Linear Viscoelastic Space Structures", Journal of Vibration and Accoustics, Vol. 115, No. 1, pp. 103-113.

Mead, D. J., 1998, "Passive Vibration Control", Wiley, Canada, pp. 554.

Nashif, A. D., Jones, D. I. G. And Henderson, J. P., 1985, "Vibration Damping", Wiley, New York, Chap. 1.